

8.6.4 Solution with Axial Conduction

Axial conduction is not commonly considered in heat exchanger analyses. However, the effect of axial conduction may be important for some heat exchangers; in particular, axial conduction is critical for very high effectiveness heat exchangers. Section 8.7 discusses the impact of axial conduction in a heat exchanger and provides several approximate models that can be used to estimate the associated performance degradation. The discussion in Section 8.7 is facilitated by the numerical model developed in this section that explicitly accounts for axial conduction. The solution technique that is discussed in Section 8.6.2, integration of the governing equations, can also be used for situations where axial conduction is important. However, the inclusion of axial conduction leads to a non-parabolic differential equation set which makes this approach more difficult. The solution technique that was discussed in Section 8.6.3, modeling the heat exchanger by breaking it into sub-heat exchangers, is not appropriate since the ε - NTU solution that is applied to each sub-heat exchanger does not account for axial conduction.

The numerical model that is developed for a heat exchanger with axial conduction is illustrated in the context of the plate heat exchanger operating in a counter-flow configuration, shown in Figure 8-43.

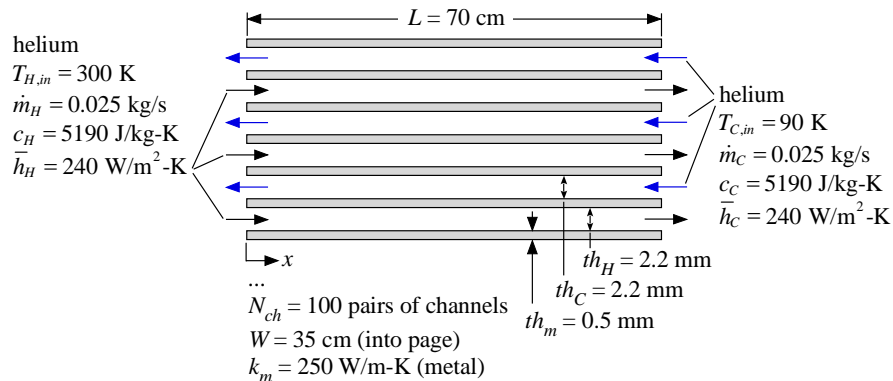


Figure 8-43: Plate heat exchanger operating in a counter-flow configuration.

The geometry of the heat exchanger is identical to the plate heat exchanger investigated in Sections 8.6.2 and 8.6.3; however, the operating conditions have changed. Helium enters the hot-side at $T_{H,in} = 300 \text{ K}$ with mass flow rate $\dot{m}_H = 0.025 \text{ kg/s}$ and helium enters the cold-side at $T_{C,in} = 90 \text{ K}$ with mass flow rate $\dot{m}_C = 0.025 \text{ kg/s}$. The specific heat capacity of helium is constant (on both sides of the heat exchanger) and equal to $c_C = c_H = 5190 \text{ J/kg-K}$. The average heat transfer coefficient on both sides is evaluated at the average temperature within the heat exchanger using the DuctFlow procedure in EES:

```
call DuctFlow('helium',(300 [K]+90 [K])/2,1000000 [Pa], 0.025 [kg/s]/100,0.0022 [m],0.35 [m],&
0.7 [m], 0 [-]:h_T, h_H, DELTAP, Nusselt_T, f, Re)
```

which leads to $\bar{h}_H = \bar{h}_C = 240 \text{ W/m}^2\text{-K}$. For the purposes of this analysis, we will assume that the local heat transfer coefficients within the heat exchanger are constant and equal to the average values, $h_H = h_C = 240 \text{ W/m}^2\text{-K}$. Because the Reynolds number is approximately 100,

E19: Section 8.6.4 *Solution with Axial Conduction*

the flow in the channels is laminar. Therefore, it is not likely that the heat transfer coefficients will change substantially with mass flow rate unless the flow rate is increased to the point where the flow condition becomes turbulent. Recall from Chapter 5 that the Nusselt number for fully developed laminar flow is constant. The conductivity of the material separating the channels is assumed to be $k_m = 250$ W/m-K and independent of temperature.

The inputs are entered in a MATLAB script:

```
% Inputs
W=0.35;           % width of heat exchanger (m)
L=0.70;           % length of heat exchanger in flow direction (m)
N_ch=100;         % number of channel pairs (-)
th_H=0.0022;      % channel width on hot-side (m)
th_C=0.0022;      % channel width on cold-side (m)
th_m=0.0005;      % thickness of plate(m)
m_dot_H=0.025;    % hot-side mass flow rate (kg/s)
m_dot_C=0.025;    % cold-side mass flow rate (kg/s)
T_H_in=300;       % hot-side inlet temperature (K)
T_C_in=90;        % cold-side inlet temperature (K)
c_H=5190;         % hot-side fluid specific heat capacity (J/kg-K)
c_C=5190;         % cold-side fluid specific heat capacity (J/kg-K)
k_m=250;          % aluminum conductivity (W/m-K)
h_H=240;          % hot-side heat transfer coefficient (W/m^2-K)
h_C=240;          % hot-side heat transfer coefficient (W/m^2-K)
```

The numerical technique proceeds by identifying control volumes and placing nodes (i.e., locations at which the temperature will be predicted) in much the same way that conduction problems are solved numerically in Chapters 1 through 3. One arrangement of nodes and control volumes is shown in Figure 8-44.

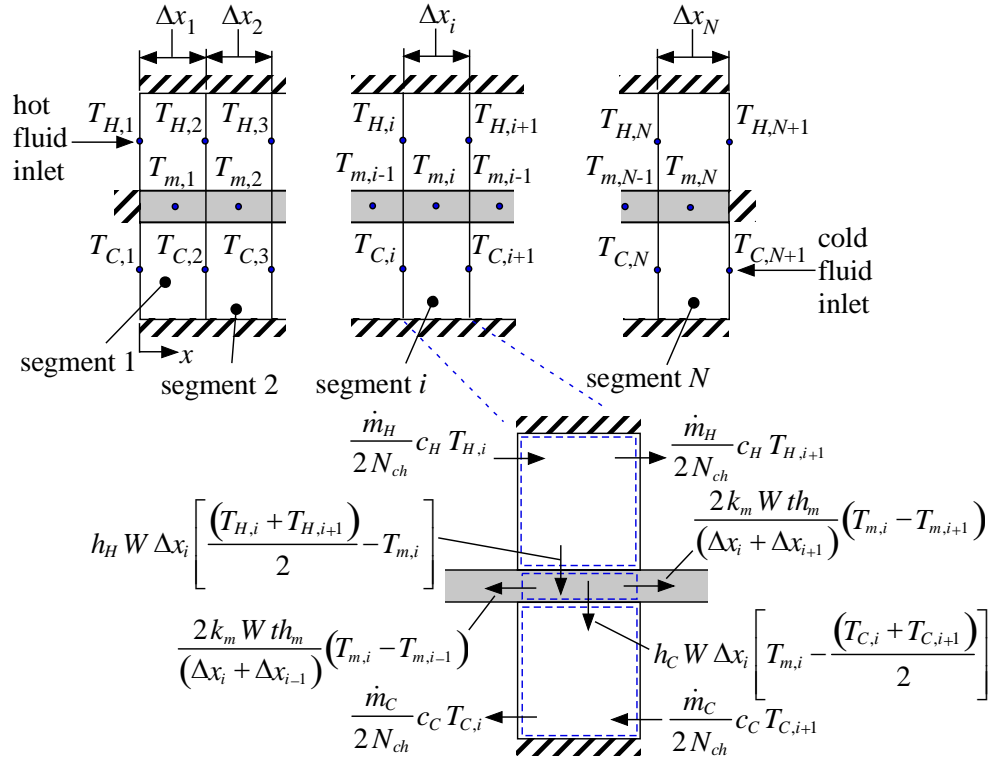


Figure 8-44: Control volumes and nodes used in numerical solution.

The numerical solution is enabled by carrying out an energy balance on each of the control volumes identified in Figure 8-44. These include control volumes that encompass the hot fluid, cold fluid, and metal within each heat exchanger section. The number of heat exchanger sections (N) is specified:

```
N=500;      % number of nodes (-)
```

The nodes must be positioned along the heat exchanger. The simplest option is to make the width of each section (Δx_i) the same:

$$\Delta x_i = \frac{L}{N} \quad \text{for } i = 1..N \quad (8-188)$$

```
for i=1:N
    DELTAX(i)=L/N;    % size of each section, uniform distribution (m)
end
```

We will see later in this section that a more optimal distribution of the nodes will concentrate them at the ends of the heat exchanger where the most interesting effects are occurring. Therefore, the program is written so that it is flexible with respect to the choice of the nodal spacing. The first fluid temperature nodes ($T_{H,1}$ and $T_{C,1}$) are placed at the hot end of the heat exchanger (see Figure 8-44):

$$x_{f,1} = 0 \quad (8-189)$$

The remaining fluid temperature nodes are distributed according to the separation distance identified in Eq. (8-188):

$$x_{f,i+1} = x_{f,i} + \Delta x_i \quad \text{for } i = 1..N \quad (8-190)$$

```
% location of fluid temperature nodes
xf(1)=0;
for i=1:N
    xf(i+1)=xf(i)+DELTAx(i);
end
```

The first metal node, $T_{m,1}$, is placed in the middle of the first control volume (see Figure 8-44):

$$x_{m,1} = \frac{\Delta x_1}{2} \quad (8-191)$$

The remaining metal temperature nodes are distributed according to the separation distance identified in Eq. (8-188):

$$x_{m,i+1} = x_{m,i} + \frac{\Delta x_i + \Delta x_{i+1}}{2} \quad \text{for } i = 1..(N-1) \quad (8-192)$$

```
% location of metal temperature nodes
xm(1)=DELTAx(1)/2;
for i=1:(N-1)
    xm(i+1)=xm(i)+(DELTAx(i)+DELTAx(i+1))/2;
end
```

The energy balances for each control volume with appropriate boundary conditions will result in a system of equations that can be solved in order to provide the temperature at each node. The solution will be implemented using MATLAB and therefore it is necessary to arrange this system of equations in a matrix form:

$$\underline{\underline{A}} \underline{\underline{X}} = \underline{\underline{b}} \quad (8-193)$$

where the vector $\underline{\underline{X}}$ contains the unknown temperatures at each node and the matrix $\underline{\underline{A}}$ and vector $\underline{\underline{b}}$ contain the coefficients multiplying the unknowns and the constants associated with each equation, respectively. In order to set up $\underline{\underline{A}}$ and $\underline{\underline{b}}$, and therefore solve Eq. (8-193) for $\underline{\underline{X}}$, it is necessary to carefully lay out the arrangement of the unknown temperatures in $\underline{\underline{X}}$ and the arrangement of the equations in $\underline{\underline{A}}$ and $\underline{\underline{b}}$. Equation (8-194) provides one possible arrangement of the unknown temperatures in $\underline{\underline{X}}$:

$$\underline{X} = \begin{bmatrix} X_1 = T_{H,1} \\ \dots \\ X_{N+1} = T_{H,N+1} \\ X_{N+1+1} = T_{C,1} \\ \dots \\ X_{2(N+1)} = T_{C,N+1} \\ X_{2(N+1)+1} = T_{m,1} \\ \dots \\ X_{2(N+1)+N} = T_{m,N} \end{bmatrix} \quad (8-194)$$

According to Eq. (8-194), the unknown temperature $T_{H,i}$ is entry i of \underline{X} . Similarly, the unknown temperature $T_{C,i}$ is entry $(N+1)+i$ of \underline{X} and the unknown temperature $T_{m,i}$ is entry $2(N+1)+i$ of \underline{X} . Equation (8-195) provides the arrangement of the equations that specifies the problem in \underline{A} and \underline{b} :

$$\underline{A} = \begin{bmatrix} \text{row 1 = hot fluid inlet temperature specification} \\ \text{row 2 = energy balance on hot-side of segment 1} \\ \dots \\ \text{row } N+1 = \text{energy balance on hot-side of segment } N \\ \text{row } (N+1)+1 = \text{energy balance on cold-side of segment 1} \\ \dots \\ \text{row } (N+1)+N = \text{energy balance on cold-side of segment } N \\ \text{row } (N+1)+N+1 = \text{cold fluid inlet temperature specification} \\ \text{row } 2(N+1)+1 = \text{energy balance on metal in segment 1} \\ \dots \\ \text{row } 2(N+1)+N = \text{energy balance on metal in segment } N \end{bmatrix} \quad (8-195)$$

According to Eq. (8-195), the hot fluid inlet boundary condition should be placed in row 1 of \underline{A} and \underline{b} and the hot-side fluid energy balances for segment i should be placed in row $i+1$ of \underline{A} and \underline{b} . Similarly, the cold-side fluid energy balances for segment i should be placed in row $(N+1)+i$ of \underline{A} and \underline{b} and the cold-side fluid inlet boundary condition is placed in row $2N+1$ of \underline{A} and \underline{b} . Finally, the energy balances on the metal in segment i should be placed in row $2(N+1)+i$ of \underline{A} and \underline{b} . The solution proceeds by filling in \underline{A} and \underline{b} from the top to the bottom according to Eqs. (8-194) and (8-195). The matrix \underline{A} and vector \underline{b} are initialized as zeros; later, we will recognize that matrix \underline{A} is sparse and reallocate it as a sparse matrix.

```
% initialize A and b
A=zeros(2*(N+1)+N,2*(N+1)+N);
b=zeros(2*(N+1)+N,1);
```

The hot fluid inlet temperature is specified:

$$T_{H,1} = T_{H,in} \quad (8-196)$$

Equation (8-196) is rearranged in order to identify the coefficients that should be placed in row 1 of $\underline{\underline{A}}$ and $\underline{\underline{b}}$:

$$T_{H,1} \underbrace{[1]}_{A_{1,1}} = \underbrace{T_{H,in}}_{b_1} \quad (8-197)$$

`% hot fluid inlet specification`

```
A(1,1)=1;
b(1)=T_H_in;
```

An energy balance on the hot-fluid in an arbitrary section i of the heat exchanger is shown in Figure 8-44 and leads to:

$$\frac{\dot{m}_H}{2 N_{ch}} c_H T_{H,i} = \frac{\dot{m}_H}{2 N_{ch}} c_H T_{H,i+1} + h_H W \Delta x_i \left[\frac{(T_{H,i} + T_{H,i+1})}{2} - T_{m,i} \right] \text{ for } i = 1..N \quad (8-198)$$

The factor of two that appears in the first two terms of Eq. (8-198) is related to the fact that the control volume on the hot fluid extends half-way across the hot fluid channel. Note that the thermal resistance of the metal in the stream-to-stream direction is assumed to be negligible relative to the convective resistance between the metal surface and the adjacent hot-fluid. Also, axial conduction in the fluid is ignored as being negligible relative to axial conduction through the metal heat exchanger structure. This assumption is valid for most fluids but may not be appropriate for fluids with very low Prandtl number (e.g., liquid metals). Equation (8-198) is rearranged in order to identify the coefficients:

$$T_{H,i} \underbrace{\left[\frac{\dot{m}_H}{2 N_{ch}} c_H - \frac{h_H W \Delta x_i}{2} \right]}_{A_{i+1,i}} + T_{H,i+1} \underbrace{\left[-\frac{\dot{m}_H}{2 N_{ch}} c_H - \frac{h_H W \Delta x_i}{2} \right]}_{A_{i+1,i+1}} + T_{m,i} \underbrace{[-h_H W \Delta x_i]}_{A_{i+1,2(N+1)+i}} = 0 \quad (8-199)$$

for $i = 1..N$

`% hot-side energy balances`

```
for i=1:N
```

```
    A(i+1,i)=m_dot_H*c_H/(2*N_ch)-h_H*W*DELTAx(i)/2;
    A(i+1,i+1)=-m_dot_H*c_H/(2*N_ch)-h_H*W*DELTAx(i)/2;
    A(i+1,2*(N+1)+i)=h_H*W*DELTAx(i);
```

```
end
```

An energy balance on the cold-side fluid in an arbitrary section i of the heat exchanger (also shown in Figure 8-44) provides:

$$\frac{\dot{m}_C}{2 N_{ch}} c_C T_{C,i+1} + h_C W \Delta x_i \left[T_{m,i} - \frac{(T_{C,i} + T_{C,i+1})}{2} \right] = \frac{\dot{m}_C}{2 N_{ch}} c_C T_{C,i} \text{ for } i = 1..N \quad (8-200)$$

which can be rearranged according to:

$$T_{C,i} \underbrace{\left[-\frac{h_c W \Delta x_i}{2} - \frac{\dot{m}_c c_c}{2 N_{ch}} \right]}_{A_{N+1+i, N+1+i}} + T_{C,i+1} \underbrace{\left[-\frac{h_c W \Delta x_i}{2} + \frac{\dot{m}_c c_c}{2 N_{ch}} \right]}_{A_{N+1+i, N+1+i+1}} + T_{m,i} \underbrace{\left[h_c W \Delta x_i \right]}_{A_{N+1+i, 2(N+1)+i}} = 0 \quad (8-201)$$

for $i = 1..N$

% cold-side energy balances

for i=1:N

```
A(N+1+i,N+1+i)=-h_c*W*DELTAx(i)/2-m_dot_C*c_C/(2*N_ch);
A(N+1+i,N+1+i+1)=-h_c*W*DELTAx(i)/2+m_dot_C*c_C/(2*N_ch);
A(N+1+i,2*(N+1)+i)=h_c*W*DELTAx(i);
```

end

The cold-side fluid inlet temperature is specified:

$$T_{C,N+1} \underbrace{\left[1 \right]}_{A_{2(N+1), 2(N+1)}} = \underbrace{T_{C,in}}_{b_{2(N+1)}} \quad (8-202)$$

% cold fluid inlet specification

```
A(N+1+N+1,N+1+N+1)=1;
b(N+1+N+1)=T_C_in;
```

An energy balance on the metal contained in node 1 of the heat exchanger leads to:

$$h_H W \Delta x_1 \left[\frac{(T_{H,1} + T_{H,2})}{2} - T_{m,1} \right] = h_c W \Delta x_1 \left[T_{m,1} - \frac{(T_{C,1} + T_{C,2})}{2} \right] + \frac{2W th_m k_m}{(\Delta x_1 + \Delta x_2)} (T_{m,1} - T_{m,2}) \quad (8-203)$$

which can be rearranged:

$$T_{H,1} \underbrace{\left[\frac{h_H W \Delta x_1}{2} \right]}_{A_{2(N+1)+1,1}} + T_{H,2} \underbrace{\left[\frac{h_H W \Delta x_1}{2} \right]}_{A_{2(N+1)+1,2}} + T_{m,1} \underbrace{\left[-h_H W \Delta x_1 - h_c W \Delta x_1 - \frac{2W th_m k_m}{(\Delta x_1 + \Delta x_2)} \right]}_{A_{2(N+1)+1, 2(N+1)+1}} +$$

$$T_{C,1} \underbrace{\left[\frac{h_c W \Delta x_1}{2} \right]}_{A_{2(N+1)+1, (N+1)+1}} + T_{C,2} \underbrace{\left[\frac{h_c W \Delta x_1}{2} \right]}_{A_{2(N+1)+1, (N+1)+2}} + T_{m,2} \underbrace{\left[\frac{2W th_m k_m}{(\Delta x_1 + \Delta x_2)} \right]}_{A_{2(N+1)+1, 2(N+1)+2}} = 0 \quad (8-204)$$

% hot end metal energy balance

```
A(2*(N+1)+1,1)=h_H*W*DELTAx(1)/2;
A(2*(N+1)+1,2)=h_H*W*DELTAx(1)/2;
A(2*(N+1)+1,2*(N+1)+1)=-h_H*W*DELTAx(1)-h_c*W*DELTAx(1)-...
2*W*th_m*k_m/(DELTAx(1)+DELTAx(2));
A(2*(N+1)+1,(N+1)+1)=h_c*W*DELTAx(1)/2;
```

$$A(2^*(N+1)+1,(N+1)+2)=h_C W \Delta x(1)/2;$$

$$A(2^*(N+1)+1,2^*(N+1)+2)=2^* W th_m k_m /(\Delta x(1)+\Delta x(2));$$

An energy balance on the metal in the internal sections (see **Error! Reference source not found.**) leads to:

$$h_H W \Delta x_i \left[\frac{(T_{H,i} + T_{H,i+1})}{2} - T_{m,i} \right] + \frac{2W th_m k_m}{(\Delta x_i + \Delta x_{i-1})} (T_{m,i-1} - T_{m,i}) =$$

$$h_C W \Delta x_i \left[T_{m,i} - \frac{(T_{C,i} + T_{C,i+1})}{2} \right] + \frac{2W th_m k_m}{(\Delta x_i + \Delta x_{i+1})} (T_{m,i} - T_{m,i+1}) \quad \text{for } i = 2..(N-1) \quad (8-205)$$

which can be rearranged:

$$T_{H,i} \underbrace{\left[\frac{h_H W \Delta x_i}{2} \right]}_{A_{2(N+1)+i,i}} + T_{H,i+1} \underbrace{\left[\frac{h_H W \Delta x_i}{2} \right]}_{A_{2(N+1)+i,i+1}} + T_{m,i-1} \underbrace{\left[\frac{2W th_m k_m}{(\Delta x_i + \Delta x_{i-1})} \right]}_{A_{2(N+1)+i,2(N+1)+i-1}} +$$

$$T_{m,i} \underbrace{\left[-h_H W \Delta x_i - \frac{2W th_m k_m}{(\Delta x_i + \Delta x_{i-1})} - h_C W \Delta x_i - \frac{2W th_m k_m}{(\Delta x_i + \Delta x_{i+1})} \right]}_{A_{2(N+1)+i,2(N+1)+i}} +$$

$$T_{C,i} \underbrace{\left[\frac{h_C W \Delta x_i}{2} \right]}_{A_{2(N+1)+i,(N+1)+i}} + T_{C,i+1} \underbrace{\left[\frac{h_C W \Delta x_i}{2} \right]}_{A_{2(N+1)+i,(N+1)+i+1}} + T_{m,i+1} \underbrace{\left[\frac{2W th_m k_m}{(\Delta x_i + \Delta x_{i+1})} \right]}_{A_{2(N+1)+i,2(N+1)+i+1}} = 0$$

for $i = 2..(N-1)$

% internal metal energy balances

for i=2:(N-1)

$$A(2^*(N+1)+i,i)=h_H W \Delta x(i)/2;$$

$$A(2^*(N+1)+i,i+1)=h_H W \Delta x(i)/2;$$

$$A(2^*(N+1)+i,2^*(N+1)+i-1)=2^* W th_m k_m /(\Delta x(i)+\Delta x(i-1));$$

$$A(2^*(N+1)+i,2^*(N+1)+i)=-h_H W \Delta x(i)-2^* W th_m k_m /(\Delta x(i)+\dots$$

$$\Delta x(i-1))-h_C W \Delta x(i)-2^* W th_m k_m /(\Delta x(i)+\Delta x(i+1));$$

$$A(2^*(N+1)+i,(N+1)+i)=h_C W \Delta x(i)/2;$$

$$A(2^*(N+1)+i,(N+1)+i+1)=h_C W \Delta x(i)/2;$$

$$A(2^*(N+1)+i,2^*(N+1)+i+1)=2^* W th_m k_m /(\Delta x(i)+\Delta x(i+1));$$

end

Finally, an energy balance on the metal in the section N leads to:

$$h_H W \Delta x_N \left[\frac{(T_{H,N} + T_{H,N+1})}{2} - T_{m,N} \right] + \frac{2W th_m k_m}{(\Delta x_N + \Delta x_{N-1})} (T_{m,N-1} - T_{m,N}) = h_C W \Delta x_N \left[T_{m,N} - \frac{(T_{C,N} + T_{C,N+1})}{2} \right] \quad (8-207)$$

which can be rearranged:

$$\begin{aligned}
 & T_{H,N} \underbrace{\left[\frac{h_H W \Delta x_N}{2} \right]}_{A_{2(N+1)+N,N}} + T_{H,N+1} \underbrace{\left[\frac{h_H W \Delta x_N}{2} \right]}_{A_{2(N+1)+N,N+1}} + T_{m,N} \underbrace{\left[-h_H W \Delta x_N - \frac{2W th_m k_m}{(\Delta x_N + \Delta x_{N-1})} - h_C W \Delta x_N \right]}_{A_{2(N+1)+N,2(N+1)+N}} + \\
 & T_{m,N-1} \underbrace{\left[\frac{2W th_m k_m}{(\Delta x_N + \Delta x_{N-1})} \right]}_{A_{2(N+1)+N,2(N+1)+N-1}} + T_{C,N} \underbrace{\left[\frac{h_C W \Delta x_N}{2} \right]}_{A_{2(N+1)+N,(N+1)+N}} + T_{C,N+1} \underbrace{\left[\frac{h_C W \Delta x_N}{2} \right]}_{A_{2(N+1)+N,(N+1)+N+1}} = 0
 \end{aligned} \tag{8-208}$$

% cold end metal energy balance

```

A(2*(N+1)+N,N)=h_H*W*DELTAx(N)/2;
A(2*(N+1)+N,N+1)=h_H*W*DELTAx(N)/2;
A(2*(N+1)+N,2*(N+1)+N)=-h_H*W*DELTAx(N)-2*W*th_m*k_m/(DELTAx(N)+...
DELTAx(N-1))-h_C*W*DELTAx(N);
A(2*(N+1)+N,2*(N+1)+N-1)=2*W*th_m*k_m/(DELTAx(N)+DELTAx(N-1));
A(2*(N+1)+N,(N+1)+N)=h_C*W*DELTAx(N)/2;
A(2*(N+1)+N,(N+1)+N+1)=h_C*W*DELTAx(N)/2;

```

The solution is obtained according to Eq. (8-193):

X=A\b; **% obtain solution**

The solution is divided into vectors containing the hot- and cold-side fluid temperatures and the metal temperatures:

% put solution into separate vectors

```

for i=1:(N+1)
    T_H(i)=X(i);
    T_C(i)=X(N+1+i);
end
for i=1:N
    T_m(i)=X(2*(N+1)+i);
end

```

Figure 8-45 illustrates the temperature distribution (the hot-side, cold-side, and metal temperature) within the heat exchanger. Notice the characteristic "temperature jumps" experienced by the hot-side and cold-side fluids as they enter the heat exchanger; these temperature jumps are discussed in Section 8.7 and they provide the basis for an approximate method that can be used to consider axial conduction.

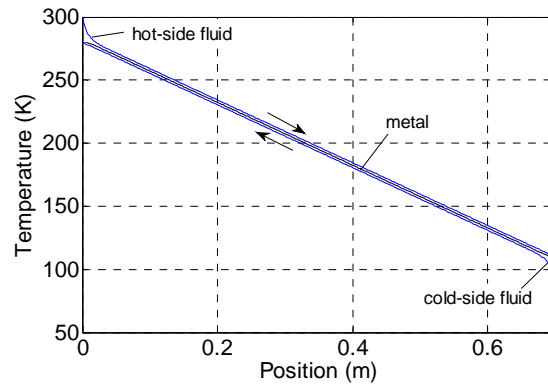


Figure 8-45: Temperature of hot- and cold-fluid and metal as a function of position.

The effectiveness of the heat exchanger can be determined based on the numerical solution. The outlet temperatures ($T_{H,out}$ and $T_{C,out}$) are identified:

```
T_H_out=T_H(N+1);           % hot outlet temperature
T_C_out=T_C(1);             % cold outlet temperature
```

The capacitance rates of the hot- and cold-side fluids are calculated:

$$\dot{C}_H = \dot{m}_H c_H \quad (8-209)$$

$$\dot{C}_C = \dot{m}_C c_C \quad (8-210)$$

```
C_dot_H=m_dot_H*c_H;       % hot-side capacitance rate
C_dot_C=m_dot_C*c_C;       % cold-side capacitance rate
```

The minimum and maximum capacitance rates (\dot{C}_{min} and \dot{C}_{max}) are identified:

```
C_dot_min=min([C_dot_H,C_dot_C]); % minimum capacitance rate
C_dot_max=max([C_dot_H,C_dot_C]); % maximum capacitance rate
```

The maximum possible rate of heat transfer in the heat exchanger is:

$$\dot{q}_{max} = \dot{C}_{min} (T_{H,in} - T_{C,in}) \quad (8-211)$$

The actual rate of heat transfer in the heat exchanger is:

$$\dot{q} = \dot{C}_H (T_{H,in} - T_{H,out}) \quad (8-212)$$

The effectiveness is:

$$\varepsilon = \frac{\dot{q}}{\dot{q}_{max}} \quad (8-213)$$

E19: Section 8.6.4 *Solution with Axial Conduction*

```
q_dot_max=C_dot_min*(T_H_in-T_C_in);    % maximum possible heat transfer rate
q_dot=C_dot_H*(T_H_in-T_H_out);        % actual heat transfer rate to hot fluid
eff=q_dot/q_dot_max;                   % effectiveness
```

which leads to $\varepsilon = 0.9018$. The program takes more time to run as the number of sections is increased. The computational speed can be improved by allocating $\underline{\underline{A}}$ as a sparse matrix; the number of nonzero elements in $\underline{\underline{A}}$ is less than 12 ($N+1$) based on examination of Eqs. (8-199), (8-201), and (8-206).

```
% initialize A and b
%A=zeros(2*(N+1)+N,2*(N+1)+N);
A=spalloc(2*(N+1)+N,2*(N+1)+N,12*(N+1));
```

Any numerical model should be verified for grid convergence and against an analytical solution in an appropriate limit. The script is converted into a function in order to facilitate these investigations and other parametric studies; the following header is added to the top of the file:

```
function[eff]=s8p6p4_f(N)

% Input:
% N – number of segments (-)

% Output:
% eff – effectiveness (-)
```

Because N is an input to the function, the specification of this parameter within the body of the function should be removed:

```
%N=500;    %number of nodes (-)
```

A script is written in order to vary the number of sections and investigate how the predicted ε converges to the actual solution.

```
clear all;
N=[2,4,6,8,10,20,30,40,50,60,80,100,120,150,200,250,300,350,400,500,600,700,800,900,1000];
for i=1:25
    [eff(i,1)]=s8p6p4_f(N(i));
end
```

Figure 8-46 illustrates the effectiveness predicted by the numerical model as a function of the number of sections.

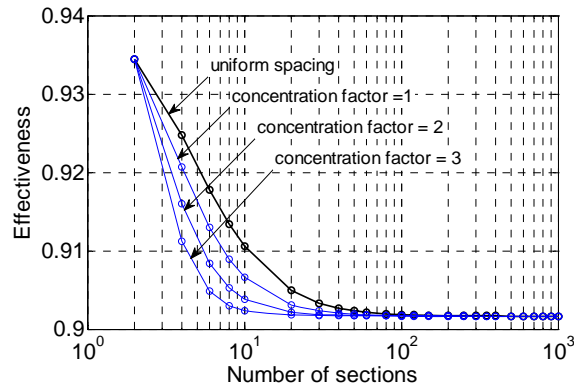


Figure 8-46: Effectiveness predicted by the numerical model using uniform and concentrated nodal spacing for various values of γ as a function of the number of nodes.

The numerical convergence can be improved by concentrating nodes towards the ends of the heat exchanger where the behavior is most interesting and important (see **Error! Reference source not found.**). One method is to use an exponentially distributed grid. The node spacing is given by:

$$\Delta x_i = \Delta x_{N+1-i} = \frac{\exp\left[-\gamma\left(1 - \frac{2i}{N}\right)\right] L}{2 \sum_1^{N/2} \exp\left[-\gamma\left(1 - \frac{2i}{N}\right)\right]} \quad \text{for } i = 1.. \frac{N}{2} \quad (8-214)$$

where γ is the concentration parameter; a larger value of γ results in a more concentrated grid, whereas $\gamma = 0$ leads to a uniform grid. The grid spacing specified by Eq. (8-188) is replaced by:

```
%for i=1:N
% DELTAX(i)=L/N; % size of each section, uniform distribution (m)
%end
gamma=1; % concentration parameter (-)
for i=1:(N/2)
    DELTAX(i)=exp(-gamma*(1-2*i/N));
    DELTAX(N+1-i)=DELTAX(i);
end
DELTAX=DELTAX*L/sum(DELTAX);
```

Figure 8-46 illustrates the effectiveness as a function of the number of segments for the concentrated grid with various values of γ and shows the advantage associated with concentrating the nodes near the ends.

The numerical solution is compared with the ε - NTU solutions discussed in Section 8.3. The capacity ratio for the heat exchanger is:

$$C_R = \frac{\dot{C}_{min}}{\dot{C}_{max}} \quad (8-215)$$

The total conductance associated with the heat exchanger is:

$$UA = \left[\frac{1}{h_H 2 N_{ch} W L} + \frac{1}{h_C 2 N_{ch} W L} \right]^{-1} \quad (8-216)$$

The number of transfer units is:

$$NTU = \frac{UA}{\dot{C}_{min}} \quad (8-217)$$

```
% no axial conduction solution
```

```
C_R=C_dot_min/C_dot_max;
```

```
% capacitance ratio
```

```
UA=1/(1/(h_H*2*N_ch*W*L)+1/(h_C*2*N_ch*W*L));
```

```
% conductance
```

```
NTU=UA/C_dot_min;
```

```
% number of transfer units
```

The ε - NTU solution for a counter-flow heat exchanger without axial conduction (ε_{nac}) is provided in Table 8-1:

$$\varepsilon_{nac} = \begin{cases} \frac{1 - \exp[-NTU(1 - C_R)]}{1 - C_R \exp[-NTU(1 - C_R)]} & \text{for } C_R < 1 \\ \frac{NTU}{1 + NTU} & \text{for } C_R = 1 \end{cases} \quad (8-218)$$

```
if(C_R~=1)
```

```
    eff_nac=(1-exp(-NTU*(1-C_R)))/(1-C_R*exp(-NTU*(1-C_R)));
```

```
else
```

```
    eff_nac=NTU/(1+NTU);
```

```
end
```

Note the use of the not equal ($\sim=$) operator in the if statement. If the capacity ratio is not equal to 1, then the ordinary formulation of the solution is provided; otherwise, the limiting solution as C_R approaches 1 is used. The header is modified so that the value of ε_{nac} is returned:

```
function[eff, eff_nac]=s8p6p4_f(N)
```

```
% Input:
```

```
% N – number of segments (-)
```

```
% Outputs:
```

```
% eff – effectiveness (-)
```

```
% eff_nac – effectiveness predicted by effectiveness-NTU solution (-)
```

In order to approach the zero conduction limit used to derive the ε - NTU solution, the value of k_m is set to a very small value:

```
%k_m=250; %aluminum conductivity (W/m-K)
```

```
k_m=0.001; % negligible conductivity to approach zero conduction limit
```

Calling the function from the workspace with a large number of sections leads to:

```
>> [eff,eff_nac]=s8p6p4_f_nu(500)
eff = 0.9784
eff_nac = 0.9784
```

which indicates that the numerical solution does appropriately limit to the ε - NTU solution when k_m becomes very small.

An EES subroutine called AxialConductionHX is provided with the EES heat exchanger library to perform the same calculations as the MATLAB program that is presented in this section. Information about the subprogram can be viewed by selecting Heat Exchangers from the pull-down menu in the Function Info dialog and then Axial Conduction from the pull-down menu of heat exchanger types.

Temperature-dependent properties (e.g., variations in the specific heat capacity, heat transfer coefficient, etc.) can be accounted for in the context of the numerical model discussed in this section. The inclusion of temperature dependent properties renders the system of equations non-linear and therefore the coefficients that are entered in \underline{A} and \underline{b} depend on temperature. The approach for solving this type of problem mirrors the solution technique presented in Section 1.5.6 for conduction problems with temperature-dependent properties. An initial guess must be made for each of the unknown temperatures and subsequently used to set up \underline{A} and \underline{b} . The solution to Eq. (8-193) is obtained and the new temperatures are used to re-evaluate \underline{A} and \underline{b} . This process is continued until the solution ceases to change significantly between iterations.